

UC San Diego

UC San Diego Previously Published Works

Title

Regulation of the Nfkbiz Gene and Its Protein Product Ikbç in Animal Models of Sepsis and Endotoxic Shock.

Permalink

<https://escholarship.org/uc/item/65j0390h>

Journal

Infection and Immunity, 89(4)

Authors

Casas, Arturo

Hawisher, Dennis

De Guzman, Christian

et al.

Publication Date

2021-03-17


DOI

10.1128/IAI.00674-20

Peer reviewed



# Regulation of the *Nfkbiz* Gene and Its Protein Product IκBζ in Animal Models of Sepsis and Endotoxic Shock

Arturo Casas, Jr.,<sup>a</sup> Dennis Hawisher,<sup>b</sup> Christian B. De Guzman,<sup>b</sup> Stephen W. Bickler,<sup>b,c</sup> Antonio De Maio,<sup>a,b,d</sup>  David M. Cauvi<sup>b</sup>

<sup>a</sup>Initiative for Maximizing Student Development Program, University of California—San Diego, La Jolla, California, USA

<sup>b</sup>Division of Trauma, Critical Care, Burns and Acute Care Surgery, Department of Surgery, School of Medicine, University of California—San Diego, La Jolla, California, USA

<sup>c</sup>Division of Pediatric Surgery, Rady Children's Hospital, San Diego, California, USA

<sup>d</sup>Department of Neurosciences, School of Medicine, University of California—San Diego, La Jolla, California, USA

**ABSTRACT** Sepsis is a life-threatening condition that arises from a poorly regulated inflammatory response to pathogenic organisms. Current treatments are limited to antibiotics, fluid resuscitation, and other supportive therapies. New targets for monitoring disease progression and therapeutic interventions are therefore critically needed. We previously reported that lipocalin-2 (*Lcn2*), a bacteriostatic mediator with potent proapoptotic activities, was robustly induced in sepsis. Other studies showed that *Lcn2* was a predictor of mortality in septic patients. However, how *Lcn2* is regulated during sepsis is poorly understood. We evaluated how IκBζ, an inducer of *Lcn2*, was regulated in sepsis using both the cecal ligation and puncture (CLP) and endotoxemia (lipopolysaccharide [LPS]) animal models. We show that *Nfkbiz*, the gene encoding IκBζ, was rapidly stimulated but, unlike *Lcn2*, whose expression persists during sepsis, mRNA levels of *Nfkbiz* decline to near basal levels several hours after its induction. In contrast, we observed that IκBζ expression remained highly elevated in septic animals following CLP but not LPS, indicating the occurrence of a CLP-specific mechanism that extends IκBζ half-life. By using an inhibitor of IκBζ, we determined that the expression of *Lcn2* was largely controlled by IκBζ. Altogether, these data indicate that the high IκBζ expression in tissues likely contributes to the elevated expression of *Lcn2* in sepsis. Since IκBζ is also capable of promoting or repressing other inflammatory genes, it might exert a central role in sepsis.

**KEYWORDS** sepsis, innate immunity, *Nfkbiz*, IκBζ, endotoxemia, IκBζ, endotoxemia, innate immunity, sepsis

Sepsis is one of the leading causes of death worldwide. In the United States, over 1.6 million patients are treated each year for sepsis representing about 6% of all hospitalizations (1, 2). Despite the use of aggressive measures, including antibiotic treatment, fluid resuscitation, and other supportive therapies, the mortality rate for sepsis is about 16% of septic patients representing more than 250,000 annual deaths (1, 2). In addition, the cost associated with the treatment of septic patients exceeds \$20 billion per year (3), which represents a tremendous financial burden on the health care system. Yet, despite extensive research, there have been no successful therapeutic treatments to improve the survival of septic patients (4).

Sepsis, recently redefined as a life-threatening organ dysfunction caused by a dysregulated host response to infection (5), progresses from an initial acute hyper-inflammatory phase to a phase of systemic immunosuppression defined by a failure of both the innate and adaptive immune systems to eradicate the initial pathogen or to mount a proper immune response against secondary infections and injuries (6). Numerous studies have suggested that this immunosuppressive phase substantially contributes to the morbidity and mortality of septic patients (7). Apoptosis of

**Citation** Casas A, Jr, Hawisher D, De Guzman CB, Bickler SW, De Maio A, Cauvi DM. 2021. Regulation of the *Nfkbiz* gene and its protein product IκBζ in animal models of sepsis and endotoxic shock. *Infect Immun* 89:e00674-20. <https://doi.org/10.1128/IAI.00674-20>.

**Editor** Denise Monack, Stanford University

**Copyright** © 2021 American Society for Microbiology. All Rights Reserved.

Address correspondence to Arturo Casas, Jr., [Arturo.CasasJr@UTSouthwestern.edu](mailto:Arturo.CasasJr@UTSouthwestern.edu), or David M. Cauvi, [dcauvi@health.ucsd.edu](mailto:dcauvi@health.ucsd.edu).

**Received** 23 October 2020

**Returned for modification** 2 December 2020

**Accepted** 28 December 2020

**Accepted manuscript posted online** 11 January 2021

**Published** 17 March 2021

various immune cells, such as B and CD4<sup>+</sup> T lymphocytes, dendritic cells, and macrophages in the spleens of septic patients, as well as in experimental animal models of sepsis, have been proposed to be significant contributors to the deregulation of the adaptive and innate immune systems in sepsis (8–11). In addition, the clearance of these apoptotic cells has been shown to exacerbate immunoparalysis by driving the inflammatory response toward an immunosuppressive phenotype (12). Understanding the mechanisms leading to these cellular changes and the subsequent systemic immunosuppression is therefore critical to improving the morbidity and mortality associated with sepsis.

We have found that lipocalin-2 (Lcn2), a bacteriostatic mediator (13–15) with potent proapoptotic activities (16–32), was rapidly and robustly induced after cecal ligation and puncture (CLP) in both C57BL/6J and A/J inbred animals, and its expression was prolonged during the immunosuppressive phase of sepsis, in contrast to most inflammatory mediators (33). Moreover, we demonstrated that the capacity to produce Lcn2 in response to lipopolysaccharide (LPS) administration during the immunosuppressive stage induced after CLP remained unaffected as opposed to the response observed for other proinflammatory cytokines (33). Studies conducted in septic patients indicated that plasma levels of Lcn2 were significantly higher in nonsurvivors than in survivors and therefore may be used as an accurate predictor of in-hospital mortality (34, 35). Based on these observations, we postulated that the excessive and sustained expression of Lcn2 during sepsis contributes to the development of the immunosuppressive phase observed as a result of this condition. This immunosuppressive condition may be related to the known capacity of Lcn2 to induce apoptosis in various cell types, including immune cells.

*Lcn2* expression is largely controlled by the NF- $\kappa$ B-mediated expression of I $\kappa$ B $\zeta$ , a member of the atypical nuclear I $\kappa$ B family of proteins (36, 37). I $\kappa$ B $\zeta$ , unlike its cytoplasmic counterparts I $\kappa$ B $\alpha$ , I $\kappa$ B $\beta$ , and I $\kappa$ B $\epsilon$ , is fully capable of inducing transcriptional activity by interacting with  $\kappa$ B or C/EBP binding sites via its association with the NF- $\kappa$ B subunits, p50 or p52 (38, 39). Once induced, I $\kappa$ B $\zeta$  either promotes or represses the expression of a set of NF- $\kappa$ B target genes, including *Lcn2* (38, 39). The induction of I $\kappa$ B $\zeta$  was found to be critical for lipopolysaccharide (LPS)-induced expression of interleukin-10 (IL-10) in macrophages (40). In addition, I $\kappa$ B $\zeta$  can also directly regulate cellular apoptosis by inhibiting the DNA binding activity of STAT3, a key transcription factor of the JAK/STAT pathway (41). The mechanisms of *Nfkbiz* (the gene encoding I $\kappa$ B $\zeta$ ) and I $\kappa$ B $\zeta$  regulation in inflammatory disorders have been mainly studied in keratinocytes in the context of psoriasis in which tumor necrosis factor alpha (TNF- $\alpha$ ) and IL-17A were described as the main inducers of this factor (42). More recently, Muller et al. showed that IL-36 was also a potent inducer of I $\kappa$ B $\zeta$  expression, as observed in biopsy specimens of psoriasis patients (43).

The mechanisms by which *Nfkbiz* mRNA levels and the expression of its resulting protein I $\kappa$ B $\zeta$  are modulated during sepsis has not yet been investigated. In the present study, we compared the kinetic expression of *Nfkbiz* and I $\kappa$ B $\zeta$  in sepsis elicited by CLP or following endotoxic shock. We found that the expression of *Nfkbiz* followed a biphasic kinetic behavior with a rapid increase within the first 3 to 6 h of CLP or endotoxic challenge and a significant decrease thereafter. In contrast, the expression I $\kappa$ B $\zeta$  kept increasing during CLP-induced sepsis but not after LPS stimulation, which seems to indicate that the stability of I $\kappa$ B $\zeta$  after CLP is extended by a mechanism that remains to be clarified. In addition, we showed that tolerized macrophages maintained their capacity to produce *Nfkbiz*, as well as various genes known to be regulated by I $\kappa$ B $\zeta$ , upon LPS restimulation. Since I $\kappa$ B $\zeta$  is not only capable of controlling the expression of *Lcn2* but also of a variety of other inflammatory genes, including IL-10 and IL-6, we propose that I $\kappa$ B $\zeta$  may be a critical, but as-yet-undefined, factor in sepsis and more predominantly during the resulting systemic immunosuppression.

## RESULTS

**Kinetic expression of *Lcn2* in various tissues of CD-1 outbred animals following CLP-induced sepsis and endotoxic challenge.** We previously found that *Lcn2* expression was strongly upregulated in the liver and lung of C57BL/6J and A/J inbred mice, detected as early as 3 h after CLP (33). For the present study, we used CD-1 outbred mice in order to better mimic the genetic variability encountered in the human population. In order to determine the expression of *Lcn2* mRNA in outbred animals in the context of polymicrobial sepsis, CD-1 mice were subjected to CLP or sham operation (sham), and various tissues were perfused and collected at different time points (3, 6, and 20 h) after surgery. Nonoperated animals were used as baseline controls (time zero). The levels of *Lcn2* mRNA in tissues were then determined by qPCR and normalized by *Gapdh* levels. The kinetic expression of *Lcn2* mRNA was similar in all tissues tested, presenting an early response (3 h), followed by a constant increase for up to 20 h after CLP (Fig. 1A). The highest induction of *Lcn2* mRNA was observed in the liver (~6,600-fold), followed by the kidney (~85-fold), at 20 h after the initial insult and to a much lesser extent in the lung and spleen (~25-fold and ~10-fold, respectively) (Fig. 1B). In accordance with our previous data (44), the kinetic expression of several other inflammatory mediators, such as *Tnfa*, *Il6*, and *Il10*, showed a biphasic pattern with an early increase within 3 to 6 h after the CLP procedure and a significant decrease thereafter (Fig. 1C). These data clearly indicate that *Lcn2* expression robustly and constantly increases during the course of CLP-induced sepsis, in contrast to the majority of inflammatory mediators. Interestingly, we found that the kinetic expression of *Lcn2* in CD-1 mice was similar to the one previously observed in C57BL/6J mice after CLP (33), as we have also recently demonstrated for the survival rate and inflammatory mediator expression (44, 45).

Next, to compare the kinetic expression of *Lcn2* during septic events caused by different challenges, CD-1 mice were treated via the intraperitoneal (i.p.) route, with 15 mg/kg of LPS dissolved in phosphate-buffered saline (PBS). Control mice received an equivalent volume of PBS, and nontreated animals were used as baseline controls (time zero). Various tissues were perfused and collected at different time points (3, 6, and 24 h) after the initial endotoxic insult. The levels of *Lcn2* mRNA in tissues were then determined by qPCR and normalized by *Gapdh* levels. The expression of *Lcn2* was also rapidly induced in all the tissues tested, but, in contrast to the data obtained following CLP, the levels of *Lcn2* mRNA significantly decreased after 3 h in the spleen and 6 h in the liver, lung, and kidney (Fig. 2A), which is consistent with the clearance of LPS in circulation (46). The liver showed the highest induction of *Lcn2* expression, whereas the spleen had the lowest (Fig. 2B), with mRNA levels reaching baseline by 24 h after LPS injection (Fig. 2A and B). Interestingly, we observed that the expression of *Tnfa*, which is mainly controlled via NF- $\kappa$ B activation, was, in contrast, highly induced in the spleen but more modestly induced in the liver (Fig. 2C). This led us to hypothesize that since the transcription of the *Tnfa* gene is rapidly induced via NF- $\kappa$ B activation following Toll-like receptor 4 (TLR4) stimulation, the *Lcn2* gene may require an additional step for its induction.

**LPS-induced expression of *Lcn2* in macrophages is associated with *Nfkbiz* activation and I $\kappa$ B $\zeta$  expression.** To test how the *Lcn2* gene is controlled at the cellular level, we first stimulated J774A.1 macrophages with LPS (10 ng/ml) for different periods of time, and the kinetic expression of *Tnfa*, *Il6*, *Il10*, and *Lcn2* genes was determined by qPCR. Control macrophages were left untreated (time zero). The expression of *Tnfa* and *Il6* rapidly increased after the LPS challenge to reach a maximal expression at 4 and 8 h, respectively, followed by a significant decrease thereafter (Fig. 3A). On the contrary, the expression of the *Il10* and *Lcn2* genes constantly increased during the 24 h of LPS challenge (Fig. 3B). Interestingly, we have previously shown that IL-10 potentiates the LPS-induced expression of *Lcn2* in macrophages (33). Next, we investigated how the *Nfkbiz* gene was regulated by LPS stimulation. We found that the kinetic expression of *Nfkbiz* was very comparable to that of *Tnfa*, suggesting a similar activation process (Fig. 3B). In parallel, we showed that the kinetic expression of *Bcl3*, another

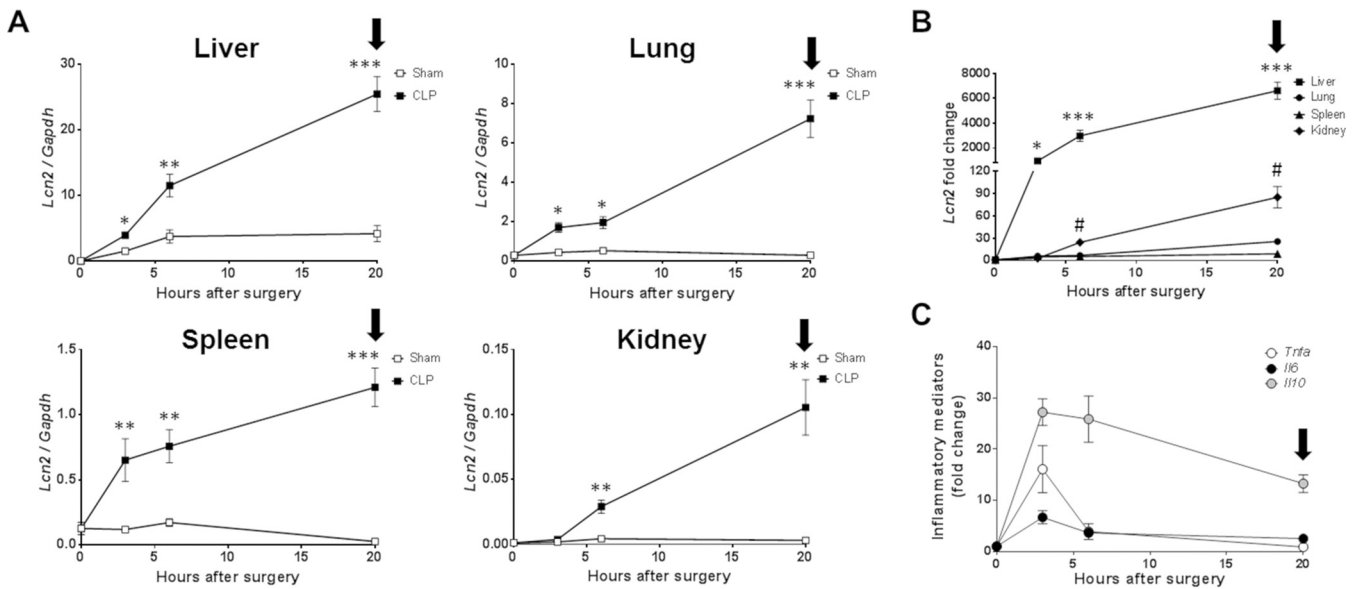


**FIG 1** Kinetic expression of *Lcn2* in tissues of CD-1 outbred mice following CLP-induced sepsis. Male CD-1 mice ( $n=5$  per time point) were subjected to sham or CLP procedure, and tissues were harvested at different time points. A nonoperated group was used to determine basal levels of *Lcn2* and as time zero for the kinetic experiment. (A) *Lcn2* gene expression in the liver, lung, spleen, and kidney was determined by qPCR at each time point by comparison with a standard curve and expressed as copy numbers. The values are expressed as the means  $\pm$  the standard errors of the mean (SEM). Statistical analysis for the time course of CLP was performed by one-way ANOVA, and the comparison between CLP and the sham operation was measured by two-way ANOVA. \*,  $P < 0.05$ ; \*\*,  $P < 0.01$ ; \*\*\*,  $P < 0.001$  (CLP versus sham-operated data at each time point). (B) Comparison of *Lcn2* gene expression in the different tissues. The data are expressed as the fold change compared to nonoperated animals, defined as 1. Statistical analysis comparing the expression of *Lcn2* between tissues at each time point was performed by two-way ANOVA. \*,  $P < 0.05$ ; \*\*\*,  $P < 0.001$  (for liver versus all other tissues). #,  $P < 0.05$  (for kidney versus all other tissues). (C) Kinetic expression of *Tnfa*, *Il6*, and *Il10* in the livers of CD-1 mice after CLP ( $n=5$  per time point). The data are expressed as the fold change compared to nonoperated animals, defined as 1. Arrows indicate the stage of immunosuppression.

member of the atypical nuclear I $\kappa$ B family of proteins, was also following the same pattern of activation (Fig. 3B). The *Nfkbiz* gene encodes the I $\kappa$ B $\zeta$  protein, which acts as a transcription factor and promotes the expression of several genes, including *Lcn2* (36). We thus tested the expression of I $\kappa$ B $\zeta$  in J774A.1 cells after LPS stimulation by Western blotting. We found that the expression of I $\kappa$ B $\zeta$  was rapidly increased but, in contrast to the *Nfkbiz* gene, I $\kappa$ B $\zeta$  expression remained elevated after 24 h of LPS challenge (Fig. 3C), while the mRNA levels decreased substantially after 4 h of LPS stimulation, which seems to indicate that the I $\kappa$ B $\zeta$  protein is rather stable.

To demonstrate the relationship between I $\kappa$ B $\zeta$  expression and *Lcn2* gene induction, we investigate whether dimethyl itaconate (DMI), an inhibitor of the I $\kappa$ B $\zeta$  protein expression (47, 48), affects the expression of *Lcn2* expression induced by LPS stimulation. We treated J774A.1 macrophages with LPS (10 ng/ml) in the presence or not of 250  $\mu$ M DMI for 24 h. We found that the expression of *Lcn2* induced by LPS was significantly reduced in the presence of DMI (Fig. 4A). This decrease in *Lcn2* expression was accompanied by a significant reduction in *Nfkbiz* mRNA levels (Fig. 4B). In contrast, levels of *Bcl3* were not affected by DMI treatment (Fig. 4B). In addition, we also measured the levels of *Tnfa*, *Il6*, and *Il10* after LPS stimulation in the presence or not of DMI. We observed that DMI treatment induced a significant increase of *Tnfa* expression compared to LPS alone (Fig. 4C). On the contrary, the expression of *Il6* and *Il10* was significantly inhibited by DMI (Fig. 4C). Interestingly, DMI treatment almost completely abolished the LPS-induced expression of *Il10* (Fig. 4C).

**LPS induces the expression of *Nfkbiz* in tolerized macrophages.** We have previously shown that tolerized macrophages maintained their capacity to produce *Lcn2* after a second LPS challenge, whereas TNF- $\alpha$  expression was completely abolished by LPS tolerization (33). If, indeed, *Lcn2* expression is regulated by I $\kappa$ B $\zeta$ , tolerized macrophages should also maintain their capacity to upregulate *Nfkbiz* expression following a second LPS challenge. J774A.1 macrophages were first incubated with either LPS (L;

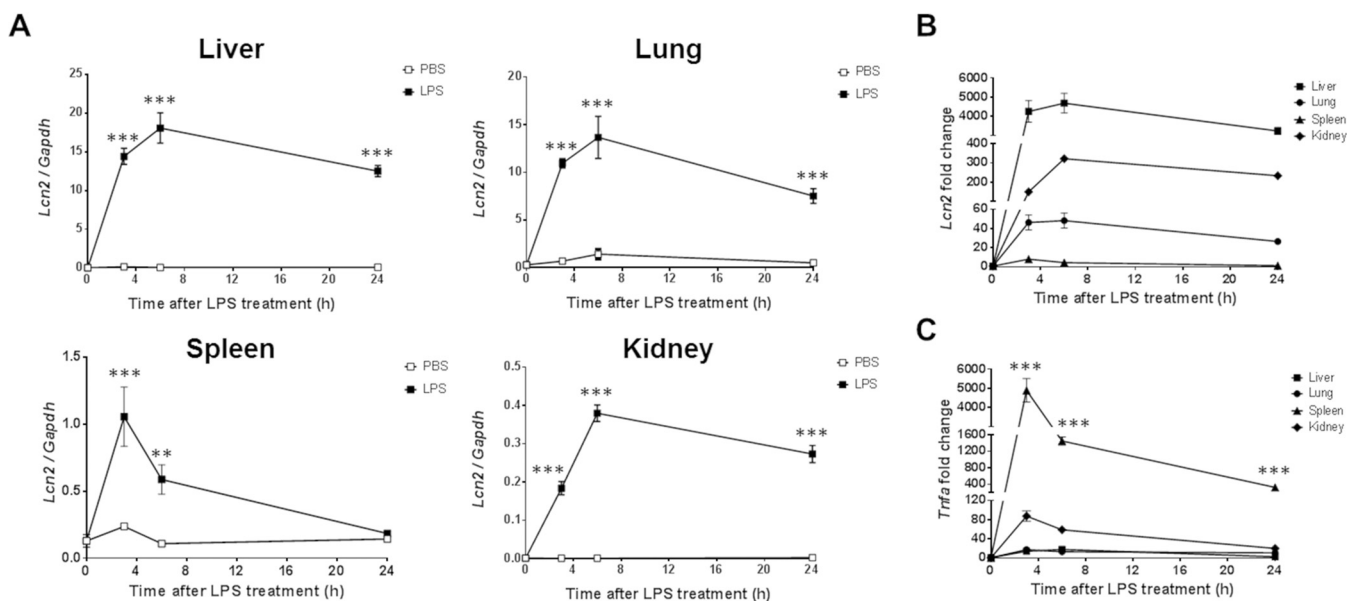


**FIG 2** Kinetic expression of *Lcn2* in tissues of CD-1 outbred mice following endotoxic challenge. Male CD-1 mice ( $n=5$  per time point) were challenged via the i.p. route with 15 mg/kg of LPS dissolved in PBS. Control mice received an equivalent volume of PBS, and nontreated animals were used as baseline controls (time zero). Tissues were harvested at different time points. (A) *Lcn2* gene expression in the liver, lung, spleen, and kidney was determined by qPCR at each time point by comparison with a standard curve and expressed as copy numbers. The values were normalized to GAPDH mRNA levels. The data are expressed as the means  $\pm$  the SEM. Statistical analysis for the time course of LPS was performed by one-way ANOVA, and comparison between LPS and PBS treatment was measured by two-way ANOVA. \*\*,  $P < 0.01$ ; \*\*\*,  $P < 0.001$  (for LPS- versus PBS-treated mice at each time point). (B) Comparison of *Lcn2* gene expression in the different tissues. The data are expressed as the fold change compared to nonoperated animals, defined as 1. Statistical analysis comparing the expression of *Lcn2* between tissues at each time point was performed by two-way ANOVA and showed that *Lcn2* expression was significantly different between all tissues at 3, 6, and 24 h postchallenge. (C) Kinetic expression of *Tnfa* in the liver, lung, spleen, and kidney of CD-1 mice after LPS ( $n=5$  per time point). The data are expressed as the fold change compared to nonoperated animals, defined as 1. Statistical analysis comparing the expression of *Tnfa* between tissues at each time point was performed by two-way ANOVA corrected for multiple comparisons by the Tukey method. \*\*\*,  $P < 0.001$  (for spleen versus all other tissues).

10 ng/ml) or not (medium, M) for 24 h. The cells were then restimulated with LPS (10 ng/ml) or not for an additional 4 h. The mRNA levels of *Lcn2*, *Nfkbiz*, *Bcl3*, *Il6*, *Csf2*, and *Csf3* were measured by qPCR. *Lcn2* expression was induced by the LPS stimulation of tolerized macrophages (L/L) to levels exceeding the one observed by a single LPS stimulation (M/L) (Fig. 5A), consistent with previous observations (33). Tolerized macrophages also maintained their capacity to produce *Nfkbiz* upon LPS restimulation, whereas *Bcl3* levels were not increased by the second LPS challenge (Fig. 5B). To confirm that I $\kappa$ B $\zeta$  was involved in the increased expression of *Lcn2* following the LPS challenge of tolerized macrophages, the expression of other inflammatory genes that are regulated by I $\kappa$ B $\zeta$ , such as *Il6*, *Csf2*, and *Csf3* (37, 43), were also analyzed. We found that these three inflammatory genes were significantly upregulated by the LPS treatment of tolerized macrophages and, for *Il6* and *Csf3*, to levels exceeding the one obtained by a single LPS treatment (Fig. 5C).

**Kinetic expression of the *Nfkbiz* gene and I $\kappa$ B $\zeta$  protein in various tissues of CD-1 outbred animals after CLP-induced sepsis and endotoxic challenge.** I $\kappa$ B $\zeta$  acts as a transcription factor capable of promoting or repressing the expression of a set of inflammatory genes (38, 39). Also, it could also directly regulate cellular apoptosis (41). However, the role of I $\kappa$ B $\zeta$  in sepsis has not yet been investigated. Indeed, only limited information is available concerning the *in vivo* regulation of the *Nfkbiz* gene and its corresponding protein, I $\kappa$ B $\zeta$ . We thus examined how the *Nfkbiz* gene was regulated after CLP. CD-1 mice were subjected to CLP or sham operation (sham), and various tissues were perfused and collected at different time points (3, 6, and 20 h) after surgery. Nonoperated animals were used as baseline controls (time zero). The levels of *Nfkbiz* mRNA in tissues were then determined by qPCR and normalized by *Gapdh* levels. In addition, we also measured the mRNA levels of *Bcl3* at the same time points. We observed that the kinetic expression of *Nfkbiz* was following the same pattern in the

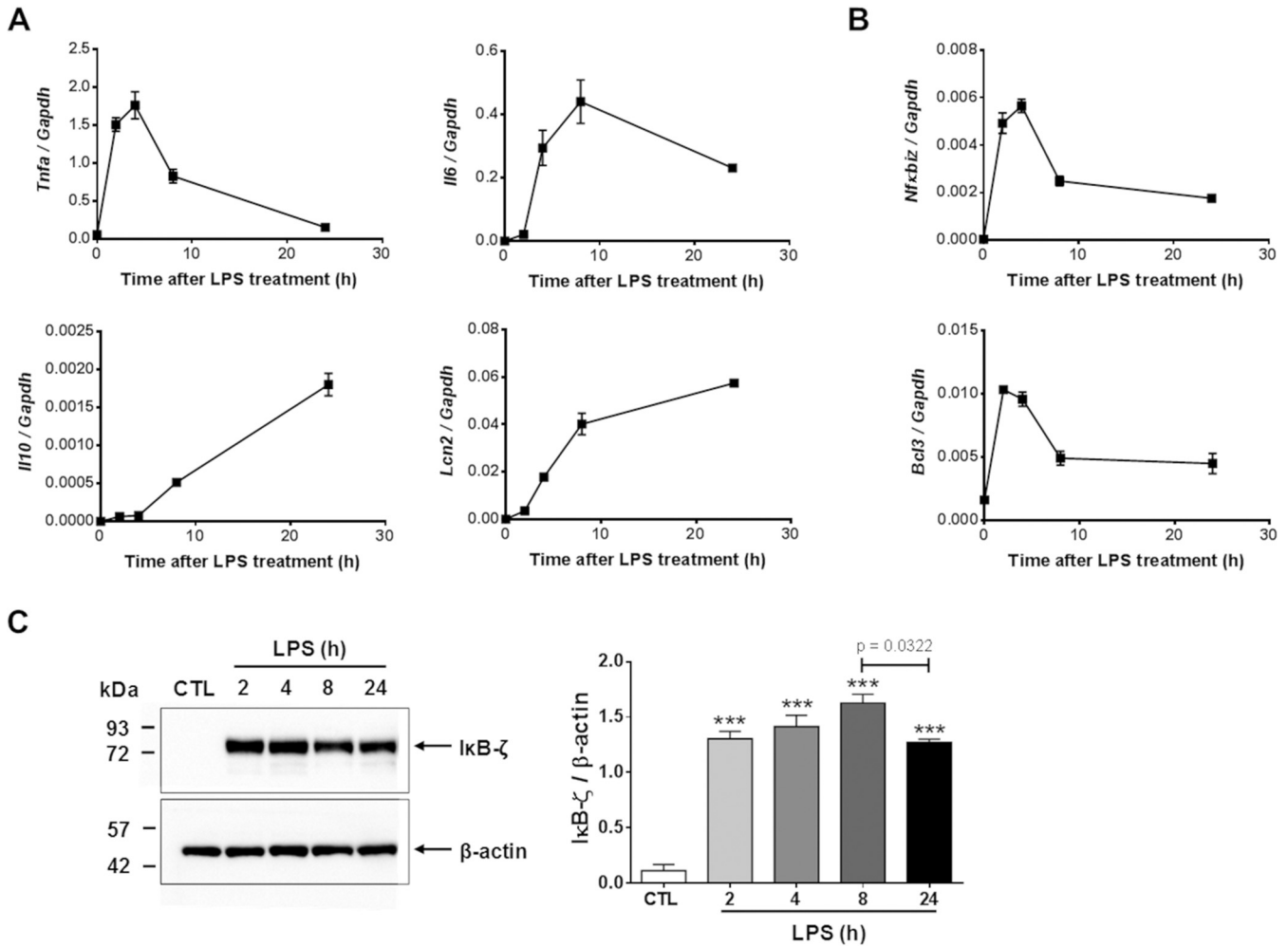


**FIG 3** Kinetic expression of *Nfkbiz* and  $I\kappa B\zeta$  in macrophages. J774A.1 macrophages were stimulated with LPS (10 ng/ml) for different periods of time ( $n=4$  per time point), and the kinetic expression of various inflammatory genes was determined by qPCR at each time point by comparison with a standard curve and expressed as copy numbers. Control macrophages were left untreated (time zero). The values were normalized to GAPDH mRNA levels. The data are expressed as the means  $\pm$  the SEM. Statistical analysis for the time course was performed by one-way ANOVA. (A) *Tnfa*, *Il6*, *Il10*, and *Lcn2* kinetic expression. (B) *Nfkbiz* and *Bcl3* kinetic expression. (C) J774A.1 macrophages were stimulated with LPS (10 ng/ml) for different periods of time, and the kinetic expression of  $I\kappa B\zeta$  was determined by Western blotting as described in Materials and Methods. A blot representative of three separate experiments is shown (left panel). Anti- $\beta$  actin antibodies were used to ensure that equivalent protein amounts were loaded in each lane. Densitometry analysis was performed using Image Lab software, and data are expressed as the means  $\pm$  the SEM (right panel). Statistical analysis was performed by one-way ANOVA corrected for multiple comparisons by the Tukey method. \*\*\*,  $P < 0.001$  (for LPS versus the control [CTL]).

liver, lung, and spleen, with a marked increase following the CLP procedure and a significant decrease between 6 and 20 h (Fig. 6A). The expression of *Nfkbiz* in the kidney increased rapidly after CLP but, in contrast to the other tissues, remained constant thereafter (Fig. 6A). As for *Lcn2*, the induction of *Nfkbiz* following CLP was the highest in the liver (Fig. 6B). The same pattern of expression was also observed for *Bcl3* but with a comparable fold of induction in all tissues (Fig. 6C). To corroborate our findings at the protein levels, we performed Western blot analysis of  $I\kappa B\zeta$  in liver samples at different time points. Interestingly, whereas the *Nfkbiz* mRNA levels significantly decreased between 6 and 20 h after CLP (Fig. 6A), the protein levels of  $I\kappa B\zeta$  continued to increase during the response (Fig. 6D), which indicates that the  $I\kappa B\zeta$  protein remains quite stable during the development of sepsis.

We next assessed the kinetic expression of *Nfkbiz* after an endotoxic challenge by treating CD-1 mice via the i.p. route with 15 mg/kg of LPS dissolved in PBS. Control mice received an equivalent volume of PBS, and nontreated animals were used as baseline controls (time zero). Various tissues were perfused and collected at different time points (3, 6, and 24 h) after the LPS challenge. Levels of *Nfkbiz* mRNA in tissues were

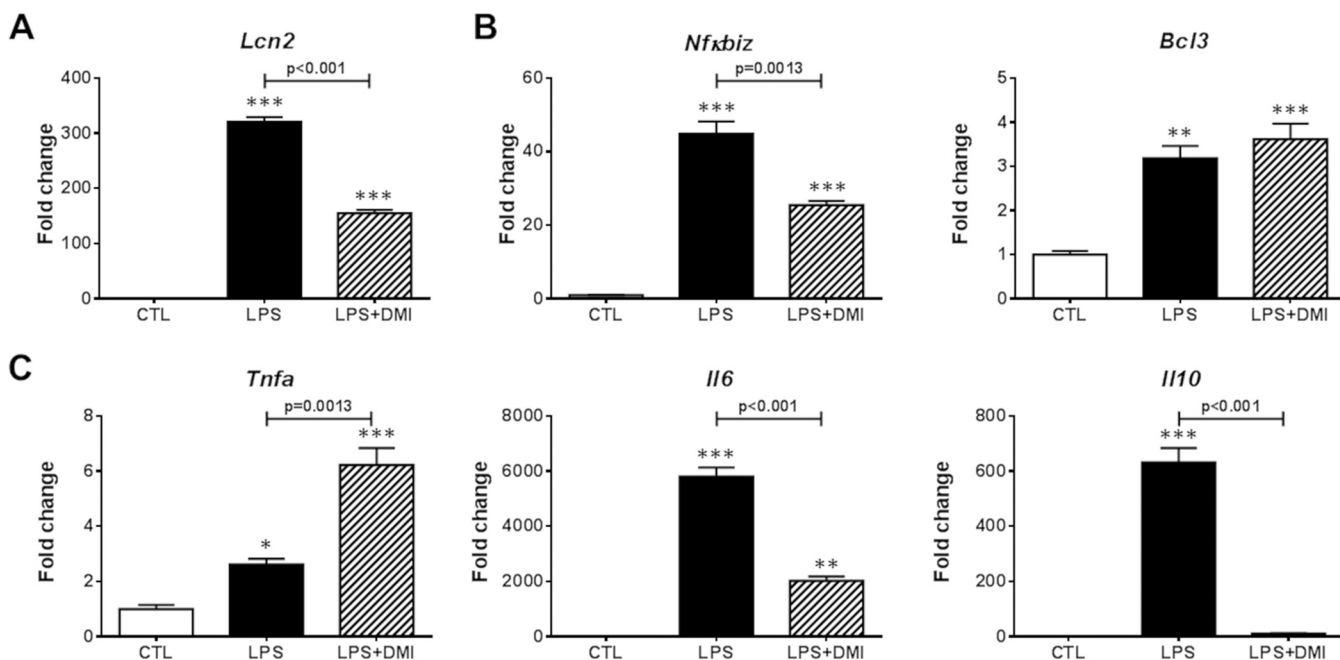


**FIG 4** Effect of DMI on the macrophage expression of *Lcn2*, *Nfkbiz*, and other inflammatory mediators. J774A.1 macrophages were treated or not with 250  $\mu$ M DMI and stimulated with LPS (10 ng/ml) for 24 h ( $n=4$ ). Control macrophages were left untreated (CTL). The expression of *Lcn2* (A), *Nfkbiz* and *Bcl3* (B), and *Tnfa*, *Il6*, and *Il10* (C) was determined by qPCR by comparison to a standard curve and is expressed as copy numbers. The values were normalized to GAPDH mRNA levels. The data are expressed as means  $\pm$  the SEM and are reported as the fold change compared to nontreated J774A.1 cells, defined as 1. Statistical analysis for the time course was performed by one-way ANOVA corrected for multiple comparisons by the Tukey method. \*,  $P < 0.05$ ; \*\*,  $P < 0.01$ ; \*\*\*,  $P < 0.001$  (for LPS or LPS+DMI versus CTL).

then determined by qPCR and normalized by *Gapdh* levels. In all tissues tested, *Nfkbiz* levels increased rapidly following the CLP procedure to reach a maximum expression at 3 h and then decreased to levels of sham-operated animals (Fig. 7A). As when following CLP, the highest induction of *Nfkbiz* expression after the endotoxic challenge was observed in the liver (Fig. 7B). Surprisingly, the LPS-induced expression of *Bcl3* was the highest in the spleen (Fig. 7C). The kinetic analysis of I $\kappa$ B $\zeta$  expression in the liver revealed that the maximum I $\kappa$ B $\zeta$  expression was reached after 6 h of LPS treatment that was followed by a sharp decrease, which is in contrast to the observations after CLP (Fig. 7D). This result implies that the stability of I $\kappa$ B $\zeta$  is quite different between the two insults.

Finally, to establish a relationship between I $\kappa$ B $\zeta$  and *Lcn2* expression *in vivo*, CD-1 mice were treated via the i.p. route with 20 mg of DMI dissolved in 500  $\mu$ l of sterile PBS as previously described (47) for 16 h before receiving 15 mg/kg of LPS. Control mice were treated with PBS for 16 h and received LPS. Liver tissue was then collected at 3 and 6 h after LPS treatment, and the *Lcn2*, *Nfkbiz*, *Bcl3*, and *Tnfa* mRNA levels were determined by qPCR. In order to ensure that DMI did not modify the cell composition of the peritoneum before LPS injection, a flow cytometry analysis of peritoneal cells was performed after 16 h of DMI treatment (see Fig. S1 in the supplemental material). The levels of *Nfkbiz* mRNA were significantly decreased in the liver of the DMI+LPS-treated group compared to the LPS only group at both time points (Fig. 8A). The expression of I $\kappa$ B $\zeta$ , monitored by Western blotting, also showed a significant decrease at both time points (Fig. 8B). The expression of *Lcn2* was reduced by DMI treatment, but this decrease only reached statistical significance at 6 h after LPS challenge (Fig. 8C). Levels of *Bcl3* were not affected by DMI, whereas the levels of *Tnfa* were increased at 6 h after LPS treatment (Fig. 8C). These data indicate that I $\kappa$ B $\zeta$  controlled, at least partially, the *in vivo* expression of *Lcn2* following a septic challenge.

## DISCUSSION

Sepsis progresses from a rapid and acute hyperinflammatory condition in response to pathogenic microorganisms to a phase of systemic immunosuppression in which the host immune system loses the capacity to eradicate the initial pathogens or to



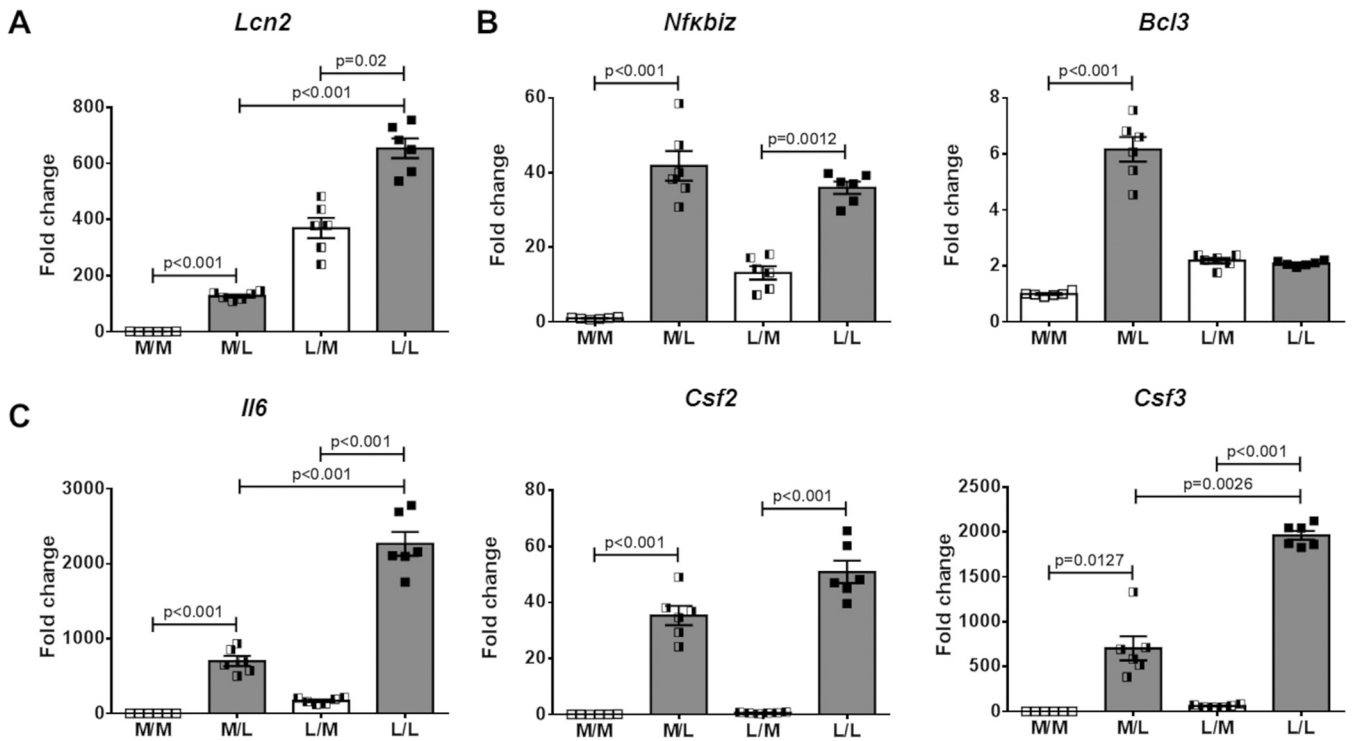


**FIG 5** LPS induces the expression of Nfkbiz in tolerized macrophages. J774A.1 cells were preincubated for 24 h with medium (M) or 10 ng/ml LPS (L), washed, and stimulated with M only or 10 ng/ml LPS for 4 h. The four conditions of stimulation are designated M/M, M/L, L/M, and L/L corresponding to pretreatment/stimulation. Total RNA was isolated, reversed, and transcribed to cDNA, and the mRNA levels were measured by qPCR for *Lcn2* (A), *Nfkbiz* and *Bcl3* (B), *Il6*, *Csf2*, and *Csf3* (C). The data are expressed as the mean  $\pm$  the SEM and are reported as the fold change compared to the M/M-treated group, defined as 1. Statistical analysis for the comparison between groups was performed by one-way ANOVA.

respond against secondary infections (6). As a consequence, numerous deaths occur during the stage of immunosuppression (49). We have previously shown in an experimental model of sepsis (CLP) that the expression of several critical inflammatory mediators showed a rapid increase after the initial injury that was followed by a drastic decrease, reaching basal levels at 20 h after CLP, prior to death (50). We also established that the response to a secondary external inflammatory stimulus (e.g., LPS) administered at a late stage (20 h) of the CLP response was compromised, supporting the concept of immune dysfunction (50). In a subsequent study, we found that the expression of *Lcn2* was rapidly and robustly induced after CLP but, in contrast to most inflammatory mediators, remained elevated at late stages of the response (33). In addition, we showed that *Lcn2* expression was further increased after a secondary inflammatory stimulus (33). Here, using an outbred strain of mice to better represent the genetic variability encountered in the human population, we found that the expression of *Lcn2* constantly increased during the course of the septic response. *Lcn2* expression levels were elevated in the liver, and to a lesser extent, in the kidney, which may imply that the main source of circulating *Lcn2* levels has a hepatic origin. The prominent circulating levels of *Lcn2* suggest that this factor could be used as a possible marker for disease severity. In this regard, circulating levels of *Lcn2* have been proposed as a potential biomarker for acute kidney injury in septic patients, which is a common complication encountered in sepsis (51). More importantly, clinical investigations concluded that the plasma levels of *Lcn2* were significantly more elevated in nonsurvivors versus survivors, suggesting that *Lcn2* could be used as a predictor of in-hospital mortality (34, 35). These observations may indicate that the higher expression of *Lcn2* found in nonsurviving septic patients and in experimental animal models, particularly at the late stage of development, may produce detrimental effects. In that regard, numerous previous studies have revealed that in addition to its bacteriostatic functions against a number of bacterial species, *Lcn2* also exerts potent proapoptotic activities in various cells, including immune cells (16–32), which is a hallmark of

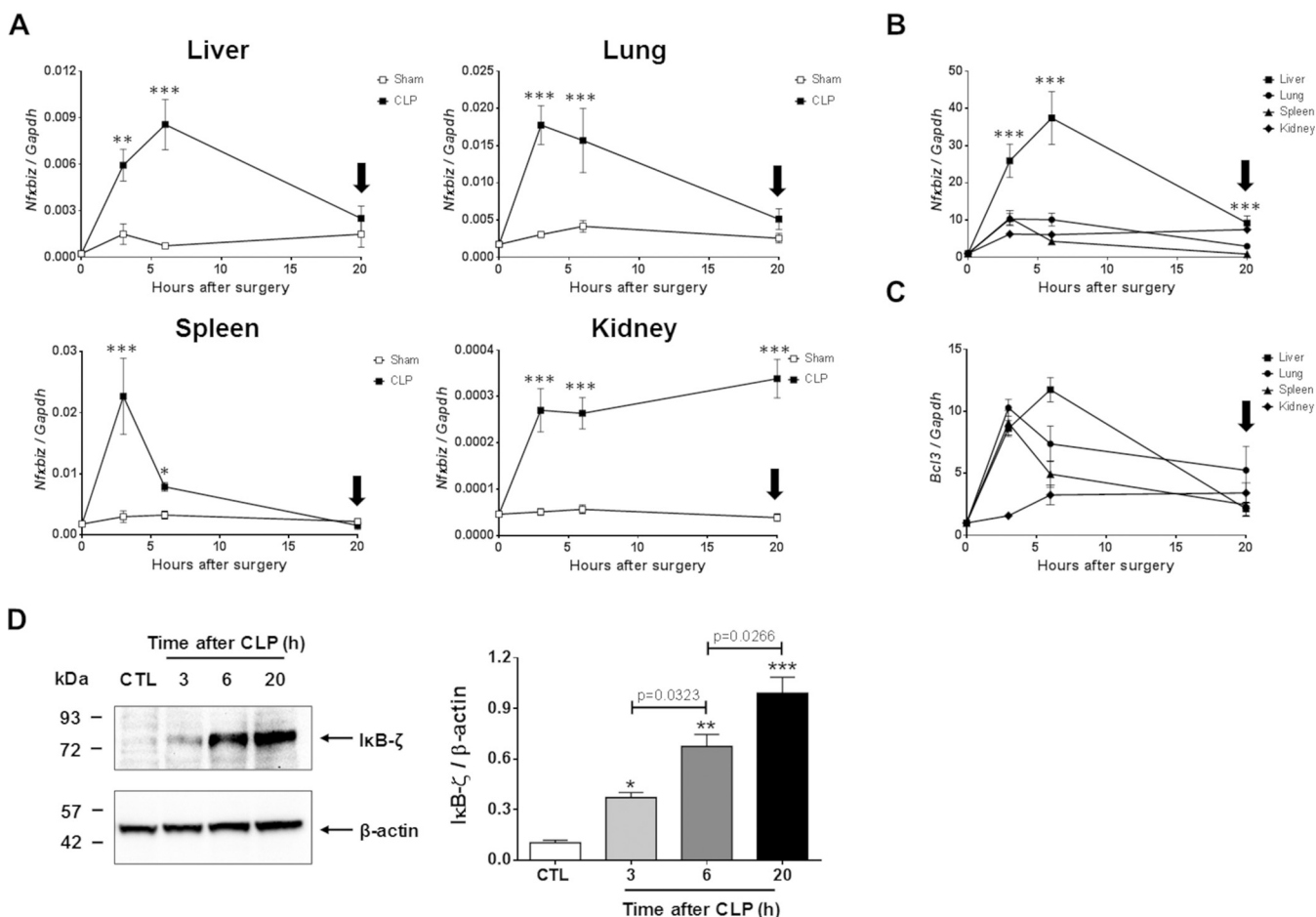


**FIG 6** Kinetic expression of *Nfkbiz* and I $\kappa$ B $\zeta$  in tissues of CD-1 outbred mice following CLP-induced sepsis. Male CD-1 mice ( $n=5$  per time point) were subjected to sham treatment or the CLP procedure, and tissues were harvested at different time points. A nonoperated group was used to determine basal levels of *Lcn2* and as time zero for the kinetic experiment. (A) *Nfkbiz* gene expression in the liver, lung, spleen, and kidney was determined by qPCR at each time point by comparison with a standard curve and expressed as copy numbers. The values were normalized to GAPDH mRNA levels. The data are expressed as the means  $\pm$  the SEM. Statistical analysis for the time course of CLP was performed by one-way ANOVA, and comparison between CLP and sham operation was measured by two-way ANOVA. \*,  $P < 0.05$ ; \*\*,  $P < 0.01$ ; \*\*\*,  $P < 0.001$  (for CLP versus sham-operated mice at each time point). (B and C) Comparison of *Nfkbiz* (B) or *Bcl3* (C) gene expression in different tissues. The data are expressed as the fold change compared to nonoperated animals, defined as 1. Statistical analysis comparing the expression of *Nfkbiz* or *Bcl3* between tissues at each time point was performed by two-way ANOVA and showed that *Lcn2* expression was significantly different between all tissues at 3, 6, and 24 h postchallenge. Arrows indicate the stage of immunosuppression. (D) Male CD-1 mice ( $n=3$  per time point) were subjected to the CLP procedure, and liver tissue was harvested at different time points. A nonoperated group (NT) was used to determine basal levels of I $\kappa$ B $\zeta$ . The kinetic expression of I $\kappa$ B $\zeta$  was determined by Western blotting as described in Materials and Methods. A blot representative of three separate experiments is shown (left panel). Anti- $\beta$  actin antibodies were used to ensure that equivalent protein amounts were loaded in each lane. Densitometry analysis was performed using Image Lab software, and the data are expressed as the means  $\pm$  the SEM (right panel). Statistical analysis was performed by one-way ANOVA corrected for multiple comparisons by the Tukey method. \*,  $P < 0.05$ ; \*\*\*,  $P < 0.001$  (for LPS versus the control [CTL]).

the systemic immunosuppression associated with sepsis and a significant risk factor for secondary infections (8–11). Moreover, other reports indicated that *Lcn2* was capable of affecting neutrophil functions by inducing neutrophil infiltration in inflamed tissues (52, 53). An increase in neutrophil recruitment within tissues combined with an abnormally high number of circulating granulocytes and delayed neutrophil apoptosis has been proposed as a mechanism of organ damage in the late stage of sepsis (52). Based on these previous studies, we postulated that *Lcn2* might indeed play a significant role in sepsis and most particularly during the associated stage of immunosuppression. Therefore, an important question that emerged was what is the mechanism for the sustained *Lcn2* expression during sepsis?

Previous reports have shown that a major contributor to *Lcn2* induction is the NF- $\kappa$ B-regulated expression of I $\kappa$ B $\zeta$ , a member of the atypical nuclear I $\kappa$ B family of proteins (36, 37). We thus examined the expression profile of *Nfkbiz* and its protein product, I $\kappa$ B $\zeta$ , in CLP. Currently, the regulation of I $\kappa$ B $\zeta$  expression in sepsis has not been investigated. We observed that the kinetic profile of *Nfkbiz* mRNA levels followed a

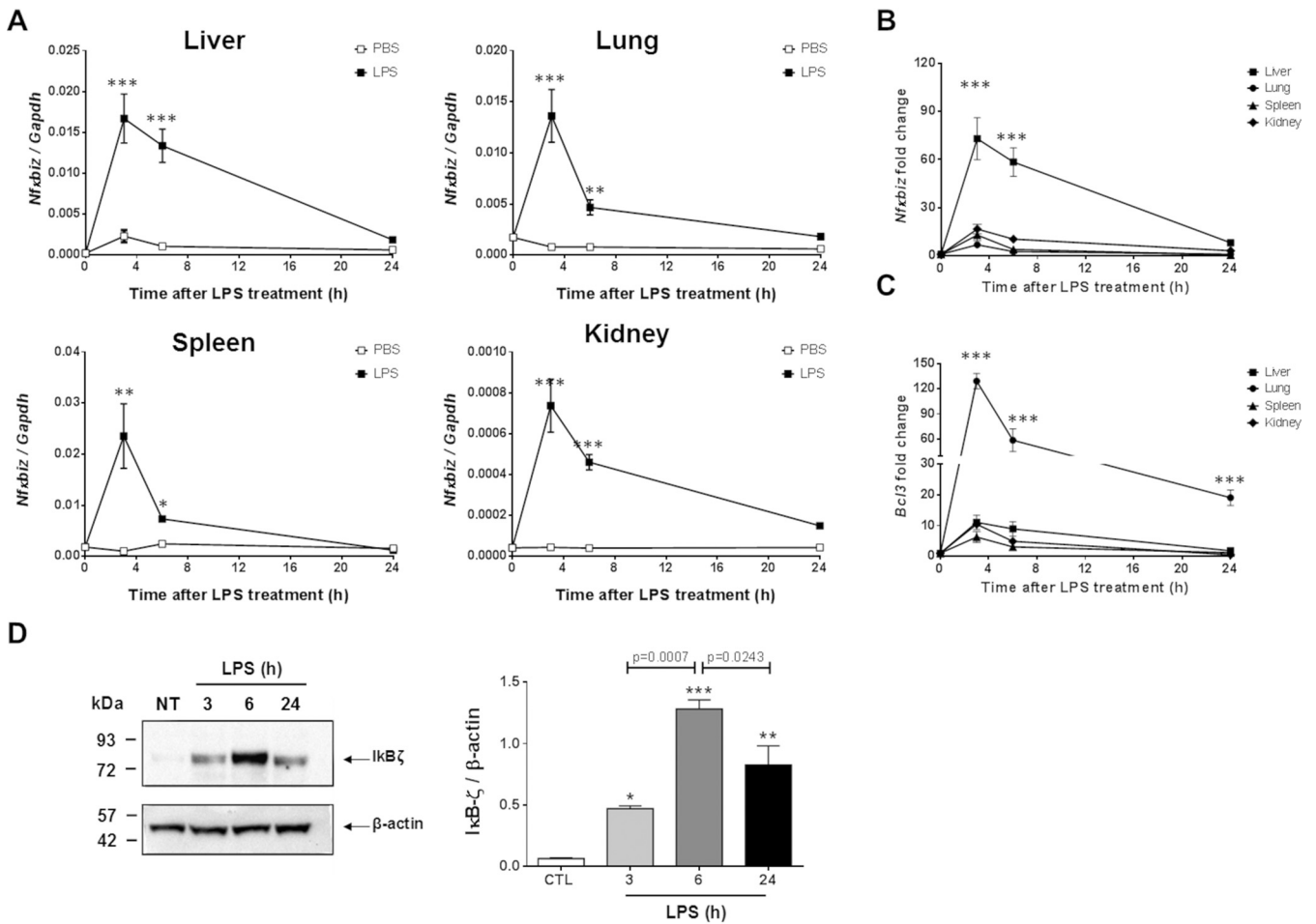


**FIG 7** Kinetic expression of *Nfkbiz* and *Ikbzeta* in tissues of CD-1 outbred mice after LPS-induced endotoxic shock. Male CD-1 mice ( $n=5$  per time point) were challenged via the i.p. route with 15 mg/kg of LPS dissolved in PBS. Control mice received an equivalent volume of PBS, and nontreated animals were used as baseline controls (time zero). Tissues were harvested at different time points. (A) *Nfkbiz* gene expression in the liver, lung, spleen, and kidney was determined by qPCR at each time point by comparison with a standard curve and is expressed as copy numbers. The values were normalized to GADPH mRNA levels. The data are expressed as the means  $\pm$  the SEM. Statistical analysis for the time course of CLP was performed by one-way ANOVA, and comparison between CLP and sham operation was measured by two-way ANOVA. \*\*,  $P < 0.01$ ; \*\*\*,  $P < 0.001$  (for LPS- versus PBS-treated mice at each time point). (B and C) Comparison of *Nfkbiz* (B) or *Bcl3* (C) gene expression in different tissues. The data are expressed as the fold change compared to nonoperated animals, defined as 1. Statistical analysis comparing the expression of *Nfkbiz* or *Bcl3* between tissues at each time point was by two-way ANOVA and showed that *Lcn2* expression was significantly different between all tissues at 3, 6, and 24 h postchallenge. (D) Male CD-1 mice ( $n=3$  per time point) were subjected to the CLP procedure, and liver tissue was harvested at different time points. A nonoperated group (NT) was used to determine the basal levels of *Ikbzeta*. The kinetic expression of *Ikbzeta* was determined by Western blotting as described in Materials and Methods. A blot representative of three separate experiments is shown (left panel). Anti- $\beta$  actin antibodies were used to ensure that equivalent protein amounts were loaded in each lane. Densitometry analysis was performed using Image Lab software, and data are expressed as the means  $\pm$  the SEM (right panel). Statistical analysis was performed by one-way ANOVA corrected for multiple comparisons by the Tukey method. \*,  $P < 0.05$ ; \*\*,  $P < 0.01$ ; \*\*\*,  $P < 0.001$  (for LPS versus control [CTL]).

biphasic pattern similar to the one previously described for many inflammatory cytokines after CLP (44, 50). Noticeably, *Nfkbiz* expression in the kidney rapidly reached a plateau after CLP and remained elevated at 20 h, which could point toward a different mechanism of *Lcn2* regulation in this tissue and may provide an explanation as to why *Lcn2* may be a good predictor of sepsis-induced acute kidney injury (51). Previous investigations have shown that *Nfkbiz* mRNA was induced by various TLR agonists, as well as by IL-1, but not by TNF- $\alpha$  (37). However, subsequent studies found that TLR agonists, IL-1, and TNF- $\alpha$  were all capable of activating the transcription of *Nfkbiz* via several kB sites located in the proximal promoter region of the gene but indicated that an additional signal, only provided by TLR agonists and IL-1 but not by TNF- $\alpha$ , was necessary for the stabilization of the *Nfkbiz* mRNA and the subsequent production of *Ikbzeta* (54). The proinflammatory IL-17 was identified as one of these secondary signals that stabilize *Nfkbiz* mRNA (55). Interestingly, we and others, have reported that IL-17A was

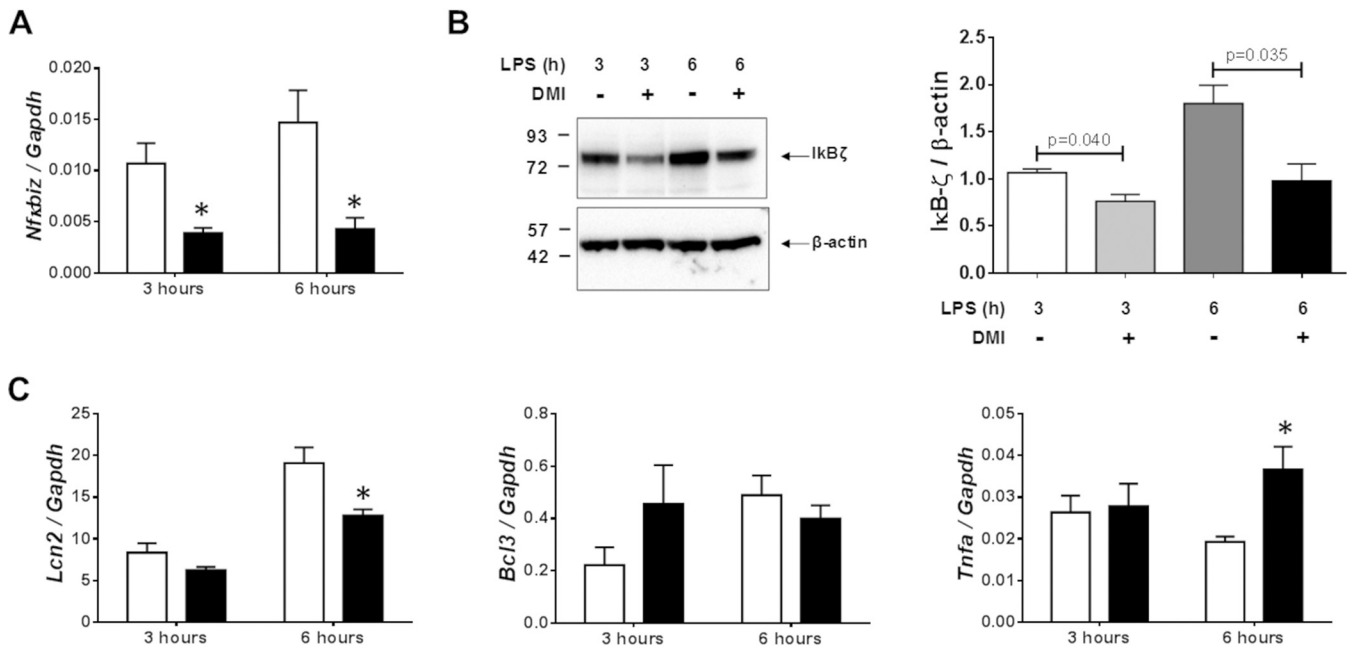


**FIG 8** DMI inhibits the *in vivo* expression of I $\kappa$ B $\zeta$  and *Lcn2* in the liver of CD-1 mice after LPS exposure. Male CD-1 mice were administered via the i.p. route with 20 mg of DMI dissolved in 500  $\mu$ l of sterile PBS or with 500  $\mu$ l of sterile PBS ( $n=8$  per treatment). After 16 h, mice were all challenged via the i.p. route with 15 mg/kg of LPS dissolved in PBS. Liver tissue was harvested at 3 and 6 h after LPS challenge ( $n=4$  per time point). (A) *Nfkbiz* gene expression in the liver was determined by qPCR at each time point by comparison with a standard curve and is expressed as copy numbers. The values were normalized to GAPDH mRNA levels. The data are expressed as the means  $\pm$  the SEM, and statistical analysis was performed by using an unpaired *t* test corrected for multiple comparisons according to the Holm-Sidak method. \*,  $P < 0.05$  (for PBS+LPS- versus DMI+LPS-treated mice at each time point). (B) Expression of I $\kappa$ B $\zeta$  was determined in PBS+LPS and DMI+LPS-treated mice at 3 and 6 h after LPS challenge by Western blotting as described in Materials and Methods. A blot representative of three separate experiments is shown (left panel). Anti- $\beta$  actin antibodies were used to ensure that equivalent protein amounts were loaded in each lane. Densitometry analysis was performed using Image Lab software, and data are expressed as the means  $\pm$  the SEM (right panel). Statistical analysis was performed by one-way ANOVA corrected for multiple comparisons by the Tukey method. (C) *Lcn2*, *Bcl3*, and *Tnfa* gene expression in the liver of PBS+LPS and DMI+LPS-treated mice at 3 and 6 h after LPS challenge was determined by qPCR at each time point by comparison with a standard curve and is expressed as copy numbers. The data are expressed as the means  $\pm$  the SEM, and statistical analysis was performed by using an unpaired *t* test corrected for multiple comparisons according to the Holm-Sidak method. \*,  $P < 0.05$  (for PBS+LPS- versus DMI+LPS-treated mice at each time point).

critical for the severity of sepsis in animal models (54, 56) and targeting IL-17A has been previously shown to significantly improve sepsis mortality after CLP (57). In contrast to our observations for *Nfkbiz* mRNA levels, we found that the expression of I $\kappa$ B $\zeta$  in the liver (the tissue showing the most *Nfkbiz* induction) increased over time after CLP suggesting that this protein accumulates in tissues during sepsis. These data indicate that, as for *Lcn2*, the expression of I $\kappa$ B $\zeta$  remained elevated at 20 h after CLP, which corresponds to the period of immune dysfunction that we have previously observed in this animal model (50) and thus suggests a potential implication of I $\kappa$ B $\zeta$  in the immunosuppressive phase of sepsis. Interestingly, whereas the kinetic of *Nfkbiz* mRNA levels in CLP-induced sepsis and after endotoxic challenge behaved in a similar manner, the I $\kappa$ B $\zeta$  expression profile differed quite significantly between the two treatments since LPS exposure did not lead to the accumulation of I $\kappa$ B $\zeta$  in the liver over time, which may be related to the short half-life of this molecule in circulation (46). These data could also suggest that additional factors may be responsible for the prolonged presence of this transcriptional factor after CLP. However, we cannot discard the possibility that changes in posttranslational modifications may affect the degradation of I $\kappa$ B $\zeta$ , extending its half-life and its accumulation. Recently, Kimura et al. reported that I $\kappa$ B $\zeta$  degradation was mediated by its association with the NAD(P)H: quinone oxidoreductase 1 (NQO1) and the PDZ and LIM domain protein-2 (PDLIM2) in a ubiquitin-dependent process (58). It is possible that this ubiquitin-mediated degradation process of I $\kappa$ B $\zeta$  is inhibited in CLP-induced sepsis but not following the LPS challenge. Dysregulation of the ubiquitin/proteasome activity in sepsis has been previously reported in skeletal muscle (59), and blocking proteasome degradation by specific inhibitors has been proposed as a treatment in septic patients (60, 61).

In addition, changes in proteasome-mediated protein degradation were also observed in the platelets of septic patients (62).

To demonstrate the relationship between I $\kappa$ B $\zeta$  expression and *Lcn2* gene induction, we used an *in vitro* system in which we stimulated macrophages with LPS for up to 24 h. While *Lcn2* and *Il10* expression showed a constant increase during these 24 h, the expression of other inflammatory cytokines such as *Tnfa* and *Il6* rapidly increased but then significantly decreased thereafter. The same kinetic behaviors were detected for two other atypical nuclear I $\kappa$ B proteins, *Nfkbiz* and *Bcl3*. Interestingly, the I $\kappa$ B $\zeta$  expression was still quite elevated at 24 h after LPS challenge, which most likely explains the kinetic of *Lcn2* expression. However, our data differed from previous reports, which showed a more transient expression of I $\kappa$ B $\zeta$  in macrophages stimulated by LPS (47, 55). This discrepancy may be a result of the type of macrophages, the culture conditions, or the amount or type of LPS used in the experiments. Our results were confirmed by the use of dimethyl itaconate (DMI), an inhibitor of the I $\kappa$ B $\zeta$  protein expression. Importantly, previous studies showed that the use of DMI at 250  $\mu$ M (this study) or at lower concentrations does not compromise the first wave of NF- $\kappa$ B activation induced by LPS (63). In good accordance with previously published data (47, 48), DMI treatment significantly inhibited *Lcn2* and *Il6* expressions but concomitantly induced an increase in *Tnfa* expression. Similar observations were made *in vivo* in the livers of CD-1 mice exposed to LPS or LPS+DMI treatment for 6 h. However, under our conditions, we found that the DMI treatment was inhibiting both the expression of I $\kappa$ B $\zeta$  and the mRNA levels of *Nfkbiz*, which contrasts with previous findings that showed only inhibition of I $\kappa$ B $\zeta$  expression but not *Nfkbiz* levels (47). The expression of TNF- $\alpha$  is mainly induced by NF- $\kappa$ B activation following TLR agonist stimulation, and the anti-inflammatory IL-10 has been shown to inhibit the transcription of TNF- $\alpha$  (64). Here, we found that DMI treatment completely abolished the expression of *Il10*, which may thus explain the DMI-induced increase in *Tnfa* expression. In addition, Horber et al. showed that I $\kappa$ B $\zeta$  controls the expression of IL-10 in macrophages and proposed that this regulatory effect of I $\kappa$ B $\zeta$  explains the chronic inflammatory phenotype observed in I $\kappa$ B $\zeta$ -deficient mice (40). Our previous study also demonstrated that IL-10 synergistically increases the LPS-induced expression of *Lcn2* (33). Collectively these data clearly indicate a relationship between I $\kappa$ B $\zeta$ , IL-10, and *Lcn2* expression during TLR-mediated inflammatory events. From these observations, we postulated that I $\kappa$ B $\zeta$  might play dual roles during sepsis. A beneficial role would be to control the initial hyperinflammatory stage of sepsis (via the anti-inflammatory activity of IL-10) and the replication of certain pathogenic bacteria (via the bacteriostatic effect of *Lcn2*). A detrimental role would be to contribute to the immunosuppressive phase by sustaining the expression of IL-10 (immunosuppressive function, (6) and *Lcn2* (as a potent proapoptotic mediator). This hypothesis is corroborated by our current and previous data showing that septic animals, during the period of immune dysfunction, or tolerized macrophages exposed to a secondary inflammatory insult were still capable of producing high levels of IL-10 and *Lcn2*, but not TNF- $\alpha$  (33, 50). Here, we found that *Nfkbiz* was also induced in LPS-tolerized macrophages by a second LPS stimulation. Several other genes, known to be controlled by *Nfkbiz*/I $\kappa$ B $\zeta$ , such as IL-6 (37), *Csf-2*, and *Csf-3* (43), were also readily stimulated in tolerized macrophages by a second LPS exposure. In contrast, the *Bcl3* gene, as it was observed for *Tnfa*, was not induced by LPS in tolerized macrophages. This potential dual role of *Nfkbiz*/I $\kappa$ B $\zeta$  in sepsis may prove that the use of *Nfkbiz* knockout mice to demonstrate how this gene influences the immunosuppressive phase of sepsis is rather challenging, since it would certainly also affect the initial phase of hyperinflammation. The use of DMI could, therefore, be of great interest, and further studies are warranted to better define the conditions of its utilization.

Altogether, these observations indicate that, in CLP-induced sepsis, the high I $\kappa$ B $\zeta$  expression found in tissues during the phase of immune dysfunction is likely the result of several mechanisms, including the induction of the *Nfkbiz* gene by TLR agonists via NF- $\kappa$ B activation, the *Nfkbiz* mRNA stabilization by inflammatory mediators such as IL-17A, and extended I $\kappa$ B $\zeta$  protein stability by a process that still needs to be identified. This elevated expression of I $\kappa$ B $\zeta$  certainly participates in the sustained expression of *Lcn2* observed in various tissues during the phase of immunosuppression, and could

thus be a significant mediator of the exaggerated apoptosis occurring in septic patients, contributing to the poor immune response to secondary infections. Finally, since I $\kappa$ B $\zeta$  has been shown to either promote or repress the expression of numerous other inflammatory genes, additional studies are needed to better define the role of this atypical nuclear I $\kappa$ B protein in sepsis. Targeting I $\kappa$ B $\zeta$  expression may therefore be envisioned as an attractive therapeutic intervention in sepsis.

## MATERIALS AND METHODS

**Animals.** Male CD-1 IGS mice (CD-1) were obtained from Charles River Laboratories (San Diego, CA) and maintained in pathogen-free conditions at the University of California—San Diego (UCSD) Animal Facility (La Jolla, CA). Experiments were conducted on 8- to 10-week-old animals and approved by the UCSD Institutional Animal Care and Use Committee.

**Cecal ligation and puncture.** Male CD-1 mice were fasted for 16 h prior to the procedure. Animals were anesthetized with isoflurane under sterile conditions, a 2-cm incision was made in the lower abdominal region, and the cecum was exposed. The distal portion of the cecum was ligated 1.5 cm from the end with a 4-0 silk suture and punctured once with a 16-gauge needle. The cecum was mobilized back into the peritoneal cavity and squeezed to place a small portion of its contents (bacteria and feces) into the peritoneum. Then, the peritoneal wall and skin were closed in two layers with silk sutures. Mice were resuscitated with a 1-ml subcutaneous injection of sterile saline (0.9%). After the procedure, mice had access to water and food *ad libitum*. As a control, mice were sham operated as described above except that the cecum was neither ligated nor perforated. Nonoperated mice were also used as a second control and used as time zero in the kinetic studies. Liver, lung, kidney, and spleen tissues were perfused to minimize polymorphonuclear leukocyte contamination and harvested at different time points after sham or CLP procedures, flash-frozen in liquid nitrogen, and then stored at  $-80^{\circ}\text{C}$  for subsequent processing.

**Endotoxin challenge.** Male CD-1 mice were injected via the i.p. route with 15 mg/kg LPS (*Escherichia coli* O26:B6; Sigma-Aldrich, St. Louis, MO) diluted in sterile PBS. Control animals received sterile PBS only. Nontreated mice were also used as a second control and used as time zero in the kinetic studies. Liver, lung, kidney, and spleen tissues were perfused to minimize polymorphonuclear leukocyte contamination and harvested at different time points after sham or CLP procedures, flash-frozen in liquid nitrogen, and then stored at  $-80^{\circ}\text{C}$  for subsequent processing. In some experiments, CD-1 mice were administered i.p. 16 h prior to the LPS injection with 20 mg of dimethyl itaconate (DMI) dissolved in 500  $\mu\text{l}$  of sterile PBS or with 500  $\mu\text{l}$  of sterile PBS, an inhibitor of the I $\kappa$ B $\zeta$  protein expression, as previously described (47). Liver tissue was perfused to minimize polymorphonuclear leukocyte contamination and harvested at 3 and 6 h after LPS injection, flash-frozen in liquid nitrogen, and then stored at  $-80^{\circ}\text{C}$  for subsequent processing.

**RNA extraction, cDNA production, and quantitative real-time PCR.** The levels of mRNA were measured by quantitative real-time PCR (qPCR). The liver, lung, kidney, and spleen tissues were homogenized in TRIzol reagent (Invitrogen, Carlsbad, CA) using an Ultra-Turrax T25 (IKA, Wilmington, NC). RNA was purified according to the manufacturer's protocol and treated with DNase I (DNA-free kit; Ambion, Austin, TX) to remove any DNA contamination. DNA-free RNA was then reverse transcribed to cDNA using a high-capacity reverse transcription kit (Applied Biosystems, Foster City, CA). Newly synthesized cDNA was further diluted and stored at  $-20^{\circ}\text{C}$ . The cDNA levels of genes were measured by quantitative real-time PCR using the QuantiTect SYBR green PCR kit (Qiagen, Valencia, CA) with QuantiTect validated primer sets (*Tnfa*, QT00104006; *Il6*, QT00098875; *Il10*, QT00106169; *Nfkbiz*, QT00143934; *Lcn2*, QT00113407; *Bcl3*, QT00247583; *Csf2*, QT00251286; *Csf3*, QT00105140 [all from Qiagen]). All PCRs were performed using the StepOnePlus real-time PCR system (Thermo Fisher Scientific). Melting curve analysis was performed for each primer set to ensure amplification specificity. Corresponding standard curves were added in each PCR. The housekeeping gene *Gapdh* (QT01658692; Qiagen) was used to normalize data to cDNA inputs. The results are expressed either as copy numbers of target gene per copy numbers of *Gapdh* or as the fold change over control as defined in each experiment.

**Macrophage J774A.1 cell line treatment.** J774A.1 cells were obtained from the American Type Culture Collection (TIB-67; ATCC, Manassas, VA). J774A.1 cells were treated with 10 ng/ml LPS (*Escherichia coli* O26:B6) for different periods of time, as indicated in each figure. Control cells received only PBS. For endotoxin tolerance experiments, J774A.1 cells were preincubated for 24 h with medium (M) or 10 ng/ml LPS (L), washed, and stimulated with medium only or 10 ng/ml LPS for an additional 4 h. The four conditions of stimulation are designated M/M, M/L, L/M, and L/L corresponding to pretreatment/stimulation. In some experiments, J774A.1 cells were treated at the time of the LPS exposure with 250  $\mu\text{M}$  DMI dissolved in sterile PBS or with 500  $\mu\text{l}$  of sterile PBS. At the end of the different treatments, cells were either harvested in TRIzol for qPCR analysis of cDNA levels as described above or lysed in RIPA buffer for I $\kappa$ B $\zeta$  expression analysis by immunoblotting as described below.

**Immunoblot analysis.** Liver samples were lysed and homogenized for 30 s in radioimmunoprecipitation assay (RIPA) lysis buffer (Abcam, Cambridge, MA) containing protease inhibitor mixture (Roche, Indianapolis, IN) using a tissue homogenizer. J774 cells were lysed in the RIPA lysis buffer and vortexed for 30 s. Liver and cell homogenates were incubated for 30 min at  $4^{\circ}\text{C}$  and sonicated for 10 s at power 15 using an ultrasonic cell disruptor. Samples were then centrifuged at  $10,000 \times g$  for 8 min at  $4^{\circ}\text{C}$ . The supernatant was collected, and a 10- $\mu\text{l}$  aliquot was used to determine protein concentration using a BCA protein assay (Pierce Biotechnology, Rockford, IL). Tissue and cell homogenates were mixed with

NuPAGE LDS sample buffer (Life Technologies, Carlsbad, CA), and 60  $\mu$ g of total protein was resolved by SDS-PAGE using NuPAGE 4–12% Bis-Tris gels (Life Technologies, Carlsbad, CA). Proteins were then transferred to nitrocellulose membranes and blocked with 5% nonfat dry milk (NFDM) diluted in Tris-buffered saline (TBS) for 1 h at 23°C. Blots were probed with a rabbit anti-I $\kappa$ B $\zeta$  polyclonal antibodies (1:1,000; Cell Signaling Technology, Beverly, MA) in 5% NFDM-TBS and incubated overnight at 4°C, followed by three 15-min washes with TBS supplemented with 0.1% Tween 20 (TBST) at 23°C. Blots were then incubated with horseradish peroxidase (HRP)-conjugated goat anti-rabbit IgG antibodies (1:2,000; Santa Cruz Biotechnology, Dallas, TX) in 5% NFDM-TBS for 1 h at 23°C. After three 15-min washes in TBST, bands were detected by chemiluminescence using SuperSignal reagents (Pierce Biotechnology). As a loading control, blots were probed with mouse anti- $\beta$ -actin monoclonal antibodies (1:3,000; Thermo Scientific, Waltham, MA) in 5% NFDM-TBS for 16 h at 4°C. Goat anti-mouse HRP-conjugated IgG secondary antibody (1:3,000; Thermo Scientific) was used for 1 h at 23°C, followed by chemiluminescence detection. Chemiluminescence data were acquired using the ChemiDoc MP system (Bio-Rad, Hercules, CA), and densitometry analyses were performed using the Image Lab software (Bio-Rad).

**Flow cytometry analysis of peritoneal cells.** Peritoneal cells were obtained by lavage of the peritoneum by injecting 5 ml of serum-free phenol-red-free RPMI 1640 into the peritoneal cavity of CD-1 mice. After a gentle massage of the peritoneum to dislodge any loosely attached cells, fluid was collected. Cells were centrifuged for 10 min at 300  $\times$  g, resuspended in PBS without Ca<sup>2+</sup>/Mg<sup>2+</sup> supplemented with 0.5% BSA (FACS staining buffer [FSB]), and counted. Peritoneal cells ( $5 \times 10^5$  cells/tube) were then incubated for 15 min with 0.5  $\mu$ g of Fc $\gamma$ R blocking antibodies (Fc block; BD Biosciences, San Jose, CA), followed by antibody staining for 30 min in the dark at 4°C. The cells were then washed, centrifuged, and resuspended in FSB for analysis. Each anti-mouse antibody was added at 0.5  $\mu$ g/tube and included fluorescein isothiocyanate-conjugated anti-Ly6G (clone 1A8; BioLegend, San Diego, CA), phycoerythrin (PE)-conjugated anti-CD11b (clone M1/70; eBioscience), PE-conjugated anti-CD19 (clone 1D3; BD Bioscience), and allophycocyanin-conjugated anti-F4/80 (clone BM8; eBioscience). Propidium iodide was also used to assess cell viability. Flow cytometry was performed using a FACSCanto II flow cytometer with FACSDiva software (BD Biosciences, San Jose, CA). The data were analyzed using FlowJo software v.10.1 (Tree Star, Ashland, OR).

**Statistical analysis.** All data were analyzed using Prism software (GraphPad, San Diego, CA). Depending on the experiment, significance was analyzed using a Student *t* test and one- or two-way analysis of variance (ANOVA) corrected by Tukey's multiple-comparison test. A *P* value of <0.05 was considered statistically significant.

## SUPPLEMENTAL MATERIAL

Supplemental material is available online only.

**SUPPLEMENTAL FILE 1**, TIF file, 0.2 MB.

## ACKNOWLEDGMENTS

This study was supported by the National Institutes of Health, NIGMS (grant R25 GM083275-10).

We thank Barbara Rho for her impeccable editorial assistance in preparing the manuscript.

## REFERENCES

- Rhee C, Dantes R, Epstein L, Murphy DJ, Seymour CW, Iwashyna TJ, Kadri SS, Angus DC, Danner RL, Fiore AE, Jernigan JA, Martin GS, Septimus E, Warren DK, Karcz A, Chan C, Menchaca JT, Wang R, Gruber S, Klompas M, for the CDC Prevention Epicenter Program. 2017. Incidence and trends of sepsis in US hospitals using clinical versus claims data, 2009–2014. *JAMA* 318:1241–1249. <https://doi.org/10.1001/jama.2017.13836>.
- Elixhauser A, Friedman B, Stranges E. 2006. Septicemia in U.S. hospitals, 2009: statistical brief #122. Healthcare Cost and Utilization Project, Rockville, MD.
- Torio CM, Moore BJ. 2006. National inpatient hospital costs: the most expensive conditions by payer, 2013: statistical brief #204. Healthcare Cost and Utilization Project, Rockville, MD.
- Marshall JC. 2014. Why have clinical trials in sepsis failed? *Trends Mol Med* 20:195–203. <https://doi.org/10.1016/j.molmed.2014.01.007>.
- Singer M, Deutschman CS, Seymour CW, Shankar-Hari M, Annane D, Bauer M, Bellomo R, Bernard GR, Chiche JD, Coopersmith CM, Hotchkiss RS, Levy MM, Marshall JC, Martin GS, Opal SM, Rubenfeld GD, van der Poll T, Vincent JL, Angus DC. 2016. The Third International Consensus definitions for sepsis and septic shock (sepsis-3). *JAMA* 315:801–810. <https://doi.org/10.1001/jama.2016.0287>.
- Hotchkiss RS, Monneret G, Payen D. 2013. Sepsis-induced immunosuppression: from cellular dysfunctions to immunotherapy. *Nat Rev Immunol* 13:862–874. <https://doi.org/10.1038/nri3552>.
- Hotchkiss RS, Monneret G, Payen D. 2013. Immunosuppression in sepsis: a novel understanding of the disorder and a new therapeutic approach. *Lancet Infect Dis* 13:260–268. [https://doi.org/10.1016/S1473-3099\(13\)70001-X](https://doi.org/10.1016/S1473-3099(13)70001-X).
- Hotchkiss RS, Tinsley KW, Swanson PE, Schmiege RE, Jr, Hui JJ, Chang KC, Osborne DF, Freeman BD, Cobb JP, Buchman TG, Karl IE. 2001. Sepsis-induced apoptosis causes progressive profound depletion of B and CD4<sup>+</sup> T lymphocytes in humans. *J Immunol* 166:6952–6963. <https://doi.org/10.4049/jimmunol.166.11.6952>.
- Hotchkiss RS, Tinsley KW, Swanson PE, Grayson MH, Osborne DF, Wagner TH, Cobb JP, Coopersmith C, Karl IE. 2002. Depletion of dendritic cells, but not macrophages, in patients with sepsis. *J Immunol* 168:2493–2500. <https://doi.org/10.4049/jimmunol.168.5.2493>.
- Tinsley KW, Grayson MH, Swanson PE, Drewry AM, Chang KC, Karl IE, Hotchkiss RS. 2003. Sepsis induces apoptosis and profound depletion of splenic interdigitating and follicular dendritic cells. *J Immunol* 171:909–914. <https://doi.org/10.4049/jimmunol.171.2.909>.
- Peck-Palmer OM, Unsinger J, Chang KC, McDonough JS, Perlman H, McDunn JE, Hotchkiss RS. 2009. Modulation of the Bcl-2 family blocks sepsis-induced depletion of dendritic cells and macrophages. *Shock* 31:359–366. <https://doi.org/10.1097/SHK.0b013e31818ba2a2>.
- Hotchkiss RS, Nicholson DW. 2006. Apoptosis and caspases regulate death and inflammation in sepsis. *Nat Rev Immunol* 6:813–822. <https://doi.org/10.1038/nri1943>.
- Flo TH, Smith KD, Sato S, Rodriguez DJ, Holmes MA, Strong RK, Akira S, Aderem A. 2004. Lipocalin 2 mediates an innate immune response to

- bacterial infection by sequestering iron. *Nature* 432:917–921. <https://doi.org/10.1038/nature03104>.
14. Berger T, Togawa A, Duncan GS, Elia AJ, You-Ten A, Wakeham A, Fong HE, Cheung CC, Mak TW. 2006. Lipocalin 2-deficient mice exhibit increased sensitivity to *Escherichia coli* infection but not to ischemia-reperfusion injury. *Proc Natl Acad Sci U S A* 103:1834–1839. <https://doi.org/10.1073/pnas.0510847103>.
  15. Wu H, Santoni-Rugiu E, Ralfkiaer E, Porse BT, Moser C, Hoiby N, Borregaard N, Cowland JB. 2010. Lipocalin-2 is protective against *Escherichia coli* pneumonia. *Respir Res* 11:96. <https://doi.org/10.1186/1465-9921-11-96>.
  16. Devireddy LR, Teodoro JG, Richard FA, Green MR. 2001. Induction of apoptosis by a secreted lipocalin that is transcriptionally regulated by IL-3 deprivation. *Science* 293:829–834. <https://doi.org/10.1126/science.1061075>.
  17. Devireddy LR, Gazin C, Zhu X, Green MR. 2005. A cell surface receptor for lipocalin 24p3 selectively mediates apoptosis and iron uptake. *Cell* 123:1293–1305. <https://doi.org/10.1016/j.cell.2005.10.027>.
  18. Lin H, Monaco G, Sun T, Ling X, Stephens C, Xie S, Belmont J, Arlinghaus R. 2005. Bcr-Abl-mediated suppression of normal hematopoiesis in leukemia. *Oncogene* 24:3246–3256. <https://doi.org/10.1038/sj.onc.1208500>.
  19. Miharada K, Hiroyama T, Sudo K, Nagasawa T, Nakamura Y. 2005. Lipocalin 2 functions as a negative regulator of red blood cell production in an autocrine fashion. *FASEB J* 19:1881–1883. <https://doi.org/10.1096/fj.05-3809fje>.
  20. Lee S, Lee J, Kim S, Park JY, Lee WH, Mori K, Kim SH, Kim IK, Suk K. 2007. A dual role of lipocalin 2 in the apoptosis and deramification of activated microglia. *J Immunol* 179:3231–3241. <https://doi.org/10.4049/jimmunol.179.5.3231>.
  21. Leng X, Lin H, Ding T, Wang Y, Wu Y, Klumpp S, Sun T, Zhou Y, Monaco P, Belmont J, Aderem A, Akira S, Strong R, Arlinghaus R. 2008. Lipocalin 2 is required for BCR-ABL-induced tumorigenesis. *Oncogene* 27:6110–6119. <https://doi.org/10.1038/ncr.2008.209>.
  22. Miharada K, Hiroyama T, Sudo K, Danjo I, Nagasawa T, Nakamura Y. 2008. Lipocalin 2-mediated growth suppression is evident in human erythroid and monocyte/macrophage lineage cells. *J Cell Physiol* 215:526–537. <https://doi.org/10.1002/jcp.21334>.
  23. Nelson AM, Zhao W, Gilliland KL, Zaenglein AL, Liu W, Thiboutot DM. 2008. Neutrophil gelatinase-associated lipocalin mediates 13-*cis* retinoic acid-induced apoptosis of human sebaceous gland cells. *J Clin Invest* 118:1468–1478. <https://doi.org/10.1172/JCI33869>.
  24. Chien MH, Ying TH, Yang SF, Yu JK, Hsu CW, Hsieh SC, Hsieh YH. 2012. Lipocalin-2 induces apoptosis in human hepatocellular carcinoma cells through activation of mitochondria pathways. *Cell Biochem Biophys* 64:177–186. <https://doi.org/10.1007/s12013-012-9370-1>.
  25. Hsin IL, Hsiao YC, Wu MF, Jan MS, Tang SC, Lin YH, Hsu CP, Ko JL. 2012. Lipocalin 2, a new GADD153 target gene, as an apoptosis inducer of endoplasmic reticulum stress in lung cancer cells. *Toxicol Appl Pharmacol* 263:330–337. <https://doi.org/10.1016/j.taap.2012.07.005>.
  26. Lee S, Lee WH, Lee MS, Mori K, Suk K. 2012. Regulation by lipocalin-2 of neuronal cell death, migration, and morphology. *J Neurosci Res* 90:540–550. <https://doi.org/10.1002/jnr.22779>.
  27. Xu G, Ahn J, Chang S, Eguchi M, Ogier A, Han S, Park Y, Shim C, Jang Y, Yang B, Xu A, Wang Y, Sweeney G. 2012. Lipocalin-2 induces cardiomyocyte apoptosis by increasing intracellular iron accumulation. *J Biol Chem* 287:4808–4817. <https://doi.org/10.1074/jbc.M111.275719>.
  28. Eller K, Schroll A, Banas M, Kirsch AH, Huber JM, Nairz M, Skvortsov S, Weiss G, Rosenkranz AR, Theurl I. 2013. Lipocalin-2 expressed in innate immune cells is an endogenous inhibitor of inflammation in murine nephrotoxic serum nephritis. *PLoS One* 8:e67693. <https://doi.org/10.1371/journal.pone.0067693>.
  29. Floderer M, Prchal-Murphy M, Vizzardelli C. 2014. Dendritic cell-secreted lipocalin2 induces CD8<sup>+</sup> T-cell apoptosis, contributes to T-cell priming and leads to a TH1 phenotype. *PLoS One* 9:e101881. <https://doi.org/10.1371/journal.pone.0101881>.
  30. El Karoui K, Viau A, Dellis O, Bagattin A, Nguyen C, Baron W, Burtin M, Brouilhet M, Heidet L, Mollet G, Druihlhe A, Antignac C, Knebelmann B, Friedlander G, Bienaime F, Gallazzini M, Terzi F. 2016. Endoplasmic reticulum stress drives proteinuria-induced kidney lesions via lipocalin 2. *Nat Commun* 7:10330. <https://doi.org/10.1038/ncomms10330>.
  31. Sung HK, Chan YK, Han M, Jahng JWS, Song E, Danielson E, Berger T, Mak TW, Sweeney G. 2017. Lipocalin-2 (NGAL) attenuates autophagy to exacerbate cardiac apoptosis induced by myocardial ischemia. *J Cell Physiol* 232:2125–2134. <https://doi.org/10.1002/jcp.25672>.
  32. Wang E, Chiou YY, Jeng WY, Lin HK, Lin HH, Chin HJ, Leo Wang CK, Yu SS, Tsai SC, Chiang CY, Cheng PH, Lin HJ, Jiang ST, Chiu ST, Hsieh-Li HM. 2017. Overexpression of exogenous kidney-specific NGAL attenuates progressive cyst development and prolongs lifespan in a murine model of polycystic kidney disease. *Kidney Int* 91:412–422. <https://doi.org/10.1016/j.kint.2016.09.005>.
  33. Vazquez DE, Nino DF, De Maio A, Cauvi DM. 2015. Sustained expression of lipocalin-2 during polymicrobial sepsis. *Innate Immun* 21:477–489. <https://doi.org/10.1177/1753425914548491>.
  34. Hong DY, Kim JW, Paik JH, Jung HM, Baek KJ, Park SO, Lee KR. 2016. Value of plasma neutrophil gelatinase-associated lipocalin in predicting the mortality of patients with sepsis at the emergency department. *Clin Chim Acta* 452:177–181. <https://doi.org/10.1016/j.cca.2015.11.026>.
  35. Wang B, Chen G, Li J, Zeng Y, Wu Y, Yan X. 2017. Neutrophil gelatinase-associated lipocalin predicts myocardial dysfunction and mortality in severe sepsis and septic shock. *Int J Cardiol* 227:589–594. <https://doi.org/10.1016/j.ijcard.2016.10.096>.
  36. Yamazaki S, Muta T, Takeshige K. 2001. A novel I $\kappa$ B protein, I $\kappa$ B- $\zeta$ , induced by proinflammatory stimuli, negatively regulates nuclear factor- $\kappa$ B in the nuclei. *J Biol Chem* 276:27657–27662. <https://doi.org/10.1074/jbc.M103426200>.
  37. Yamamoto M, Yamazaki S, Uematsu S, Sato S, Hemmi H, Hoshino K, Kaisho T, Kuwata H, Takeuchi O, Takeshige K, Saitoh T, Yamaoka S, Yamamoto N, Yamamoto S, Muta T, Takeda K, Akira S. 2004. Regulation of Toll/IL-1-receptor-mediated gene expression by the inducible nuclear protein I $\kappa$ B $\zeta$ . *Nature* 430:218–222. <https://doi.org/10.1038/nature02738>.
  38. Annemann M, Plaza-Sirvent C, Schuster M, Katsoulis-Dimitriou K, Kliche S, Schraven B, Schmitz I. 2016. Atypical I $\kappa$ B proteins in immune cell differentiation and function. *Immunol Lett* 171:26–35. <https://doi.org/10.1016/j.imlet.2016.01.006>.
  39. Willems M, Dubois N, Musumeci L, Bours V, Robe PA. 2016. I $\kappa$ B $\zeta$ : an emerging player in cancer. *Oncotarget* 7:66310–66322. <https://doi.org/10.18632/oncotarget.11624>.
  40. Horber S, Hildebrand DG, Lieb WS, Lorscheid S, Hailfinger S, Schulze-Osthoff K, Essmann F. 2016. The atypical inhibitor of NF- $\kappa$ B, I $\kappa$ B $\zeta$ , controls macrophage interleukin-10 expression. *J Biol Chem* 291:12851–12861. <https://doi.org/10.1074/jbc.M116.718825>.
  41. Wu Z, Zhang X, Yang J, Wu G, Zhang Y, Yuan Y, Jin C, Chang Z, Wang J, Yang X, He F. 2009. Nuclear protein I $\kappa$ B-zeta inhibits the activity of STAT3. *Biochem Biophys Res Commun* 387:348–352. <https://doi.org/10.1016/j.bbrc.2009.07.023>.
  42. Johansen C, Mose M, Ommen P, Bertelsen T, Vinter H, Hailfinger S, Lorscheid S, Schulze-Osthoff K, Iversen L. 2015. I $\kappa$ B $\zeta$  is a key driver in the development of psoriasis. *Proc Natl Acad Sci U S A* 112:E5825–33. <https://doi.org/10.1073/pnas.1509971112>.
  43. Muller A, Hennig A, Lorscheid S, Grondda P, Schulze-Osthoff K, Hailfinger S, Kramer D. 2018. I $\kappa$ B $\zeta$  is a key transcriptional regulator of IL-36-driven psoriasis-related gene expression in keratinocytes. *Proc Natl Acad Sci U S A* 115:10088–10093. <https://doi.org/10.1073/pnas.1801377115>.
  44. Halbach JL, Wang AW, Hawisher D, Cauvi DM, Lizardo RE, Rosas J, Reyes T, Escobedo O, Bickler SW, Coimbra R, De Maio A. 2017. Why antibiotic treatment is not enough for sepsis resolution: an evaluation in an experimental animal model. *Infect Immun* 85:e00664-17. <https://doi.org/10.1128/IAI.00664-17>.
  45. Halbach JL, Prieto JM, Wang AW, Hawisher D, Cauvi DM, Reyes T, Okerblom J, Ramirez-Sanchez I, Villarreal F, Patel HH, Bickler SW, Perdrizet GA, De Maio A. 2019. Early hyperbaric oxygen therapy improves survival in a model of severe sepsis. *Am J Physiol Regul Integr Comp Physiol* 317:R160–R168. <https://doi.org/10.1152/ajpregu.00083.2019>.
  46. Fuentes JM, Talamini MA, Fulton WB, Hanly EJ, Aurora AR, De Maio A. 2006. General anesthesia delays the inflammatory response and increases survival for mice with endotoxemic shock. *Clin Vaccine Immunol* 13:281–288. <https://doi.org/10.1128/CVI.13.2.281-288.2006>.
  47. Bambouskova M, Gorvel L, Lampropoulou V, Sergushichev A, Loginicheva E, Johnson K, Korenfeld D, Mather ME, Kim H, Huang LH, Duncan D, Bregman H, Keskin A, Santeford A, Apte RS, Sehgal R, Johnson B, Amarasinghe GK, Soares MP, Satoh T, Akira S, Hai T, de Guzman Strong C, Auclair K, Roddy TP, Biller SA, Jovanovic M, Klechevsky E, Stewart KM, Randolph GJ, Artyomov MN. 2018. Electrophilic properties of itaconate and derivatives regulate the I $\kappa$ B $\zeta$ -ATF3 inflammatory axis. *Nature* 556:501–504. <https://doi.org/10.1038/s41586-018-0052-z>.
  48. Swain A, Bambouskova M, Kim H, Andhey PS, Duncan D, Auclair K, Chubukov V, Simons DM, Roddy TP, Stewart KM, Artyomov MN. 2020. Comparative evaluation of itaconate and its derivatives reveals divergent



- inflammasome and type I interferon regulation in macrophages. *Nat Metab* 2:594–602. <https://doi.org/10.1038/s42255-020-0210-0>.
49. Chang DW, Tseng CH, Shapiro MF. 2015. Rehospitalizations following sepsis: common and costly. *Crit Care Med* 43:2085–2093. <https://doi.org/10.1097/CCM.0000000000001159>.
  50. Cauvi DM, Song D, Vazquez DE, Hawisher D, Bermudez JA, Williams MR, Bickler S, Coimbra R, De Maio A. 2012. Period of irreversible therapeutic intervention during sepsis correlates with phase of innate immune dysfunction. *J Biol Chem* 287:19804–19815. <https://doi.org/10.1074/jbc.M112.359562>.
  51. Md Ralib A, Mat Nor MB, Pickering JW. 2017. Plasma neutrophil gelatinase-associated lipocalin diagnosed acute kidney injury in patients with systemic inflammatory disease and sepsis. *Nephrology* 22:412–419. <https://doi.org/10.1111/nep.12796>.
  52. Schroll A, Eller K, Feistritz C, Nairz M, Sonnweber T, Moser PA, Rosenkranz AR, Theurl I, Weiss G. 2012. Lipocalin-2 ameliorates granulocyte functionality. *Eur J Immunol* 42:3346–3357. <https://doi.org/10.1002/eji.201142351>.
  53. Shao S, Cao T, Jin L, Li B, Fang H, Zhang J, Zhang Y, Hu J, Wang G. 2016. Increased lipocalin-2 contributes to the pathogenesis of psoriasis by modulating neutrophil chemotaxis and cytokine secretion. *J Invest Dermatol* 136:1418–1428. <https://doi.org/10.1016/j.jid.2016.03.002>.
  54. Flierl MA, Rittirsch D, Gao H, Hoesel LM, Nadeau BA, Day DE, Zetoune FS, Sarma JV, Huber-Lang MS, Ferrara JL, Ward PA. 2008. Adverse functions of IL-17A in experimental sepsis. *FASEB J* 22:2198–2205. <https://doi.org/10.1096/fj.07-105221>.
  55. Yamazaki S, Muta T, Matsuo S, Takeshige K. 2005. Stimulus-specific induction of a novel nuclear factor- $\kappa$ B regulator, I $\kappa$ B- $\zeta$ , via Toll/Interleukin-1 receptor is mediated by mRNA stabilization. *J Biol Chem* 280:1678–1687. <https://doi.org/10.1074/jbc.M409983200>.
  56. Cauvi DM, Williams MR, Bermudez JA, Armijo G, De Maio A. 2014. Elevated expression of IL-23/IL-17 pathway-related mediators correlates with exacerbation of pulmonary inflammation during polymicrobial sepsis. *Shock* 42:246–255. <https://doi.org/10.1097/SHK.0000000000000207>.
  57. Li J, Zhang Y, Lou J, Zhu J, He M, Deng X, Cai Z. 2012. Neutralization of peritoneal IL-17A markedly improves the prognosis of severe septic mice by decreasing neutrophil infiltration and proinflammatory cytokines. *PLoS One* 7:e46506. <https://doi.org/10.1371/journal.pone.0046506>.
  58. Kimura A, Kitajima M, Nishida K, Serada S, Fujimoto M, Naka T, Fujii-Kuriyama Y, Sakamoto S, Ito T, Handa H, Tanaka T, Yoshimura A, Suzuki H. 2018. NQO1 inhibits the TLR-dependent production of selective cytokines by promoting I $\kappa$ B- $\zeta$  degradation. *J Exp Med* 215:2197–2209. <https://doi.org/10.1084/jem.20172024>.
  59. Tiao G, Hobler S, Wang JJ, Meyer TA, Luchette FA, Fischer JE, Hasselgren PO. 1997. Sepsis is associated with increased mRNAs of the ubiquitin-proteasome proteolytic pathway in human skeletal muscle. *J Clin Invest* 99:163–168. <https://doi.org/10.1172/JCI119143>.
  60. Hobler SC, Tiao G, Fischer JE, Monaco J, Hasselgren PO. 1998. Sepsis-induced increase in muscle proteolysis is blocked by specific proteasome inhibitors. *Am J Physiol* 274:R30–R37. <https://doi.org/10.1152/ajpregu.1998.274.1.R30>.
  61. Brun J, Gray DA. 2009. Targeting the ubiquitin proteasome pathway for the treatment of septic shock in patients. *Crit Care* 13:311. <https://doi.org/10.1186/cc7946>.
  62. Lopez V, Cauvi DM, Arispe N, De Maio A. 2016. Bacterial Hsp70 (DnaK) and mammalian Hsp70 interact differently with lipid membranes. *Cell Stress Chaperones* 21:609–616. <https://doi.org/10.1007/s12192-016-0685-5>.
  63. O'Neill LAJ, Artyomov MN. 2019. Itaconate: the poster child of metabolic reprogramming in macrophage function. *Nat Rev Immunol* 19:273–281. <https://doi.org/10.1038/s41577-019-0128-5>.
  64. Smallie T, Ricchetti G, Horwood NJ, Feldmann M, Clark AR, Williams LM. 2010. IL-10 inhibits transcription elongation of the human TNF gene in primary macrophages. *J Exp Med* 207:2081–2088. <https://doi.org/10.1084/jem.20100414>.